Anal. Bioanal. Electrochem., Vol. 10, No. 10, 2018, 1375-1398

Analytical & Bioanalytical Electrochemistry

2018 by CEE
www.abechem.com

Full Paper

Corrosion Inhibition Study of 5, 5-diphenylimidazolidine-2, 4-dione for Mild Steel Corrosion in 1 M HCl Solution: Experimental, Theoretical Computational and Monte Carlo Simulations Studies

Rajae Nabah[1,2], Fouad Benhiba[1,*], Youssef Ramli[3], Moussa Ouakki[2], Mohammed Cherkaoui[2], Hassan Oudda[1], Rachid Touir[4,5], Ismail Warad[6] and Abdelkader Zarrouk[7]

[1]Laboratory of Separation Processes, Faculty of Science, University IbnTofail PO Box 242, Kenitra, Morocco
[2]Laboratory of Matériaux, Electrochimie and Environnement, Faculty of Science, University IbnTofail PO Box 242, Kenitra, Morocco
[3]Laboratory of Medicinal Chemistry, Faculty of Medicine and Pharmacy, Mohammed V University Rabat, 10170 Rabat, Morocco
[4]Laboratory of Materials Engineering and Environment: Modeling and Application, Faculty of Science, University Ibn Tofail BP. 133-14000, Kenitra, Morocco
[5]Centre Régional des métiers de l'éducation et de la formation (CRMEF), Avenue Allal Al Fassi, Madinat Al Irfane, BP 6210 Rabat, Morocco
[6]Department of Chemistry, Science College, An-Najah National University, P.O. Box 7, Nablus, Palestine
[7]LC2AME, Faculty of Science, First Mohammed University, PO Box 717, 60 000 Oujda, Morocco

*Corresponding Author, Tel.: +212672605899
E-Mail: benhibafouad@gmail.com

Received: 14 July 2018 / Received in revised form: 3 August 2018 / Accepted: 11 August 2018 / Published online: 31 October 2018

Abstract- The compound ability of 5,5-diphenylimidazolidine-2,4-dione (PID) against mild steel corrosion in 1 M HCl solution was investigated by various techniques. It is found that this compound is an effective inhibitor against corrosion which its inhibition efficiency increases with its concentration. The potentiodynamic polarization curves indicated that PID acts as mixed inhibitor. In addition, these results were confirmed by the electrochemical impedance spectroscopy where the resistance transfer of PID increases by its concentration.

Thus, the inhibitor adsorption which is studied on the mild steel surface conforms to the Langmuir adsorption isotherm. On the other hand, the quantum chemical parameters were calculated by using the density functional theory (DFT) method with the 6-31G/B3LYP base (d, p) and Monte Carlo simulation. It is shown that PID adsorbs in parallel ways on the metal surface of low energy iron. Finally, the correlation between theoretical and experimental results is in good agreement.

Keywords- Mild steel, Medium HCl, Corrosion inhibition, Electrochemical Technique, DFT, Monte Carlo Simulation

1. INTRODUCTION

Corrosion inhibition study of metal surfaces against corrosion in acidic solutions by inhibitors is one of the most important industrial subjects and it is a very powerful research subject. An inhibitor is a chemical compound that has added a small amount to the corrosive medium to significantly reduce the corrosion kinetics of steel [1-3]. Organic compounds are good inhibitors of electrochemical corrosion of metals [4]. These organic compounds contain heteroatoms such as phosphorus, sulfur, nitrogen and oxygen, and aromatic rings in their structures [5-11]. These important characteristics can determine the adsorption centers of the inhibitor on the metal surface and separate the effective inhibitors from the others [12,13].

In the present work, the effect of 5, 5-diphenylimidazolidine-2,4-dione (PID) on mild steel corrosion in 1 M HCl using weight loss and electrochemical measurements. The kinetic activation parameters of the corrosion inhibition process are also evaluated. This experimental evaluation was coupled with a theoretical study using DFT method and the Monte Carlo simulation.

2. THE EXPERIMENTAL PART

2.1. Materials and the solution

The mild steel which is used in this study is an ordinary steel whose its chemical composition (wt. %) is 0.11% C, 0.24% Si, 0.47% Mn, 0.12% Cr, 0.02% Mo, 0.1% Ni, 0.03% Al, 0.14% Cu, 0.0012% Co, 0.003% V, 0.06% W and Fe Balance. The samples are prepared before each immersion, by polishing with emery paper with granulometry from 180 to 1200, in a parallel manner and similar, followed by rinsing with distilled water and then rinsing with acetone in order to remove the treatment products and finally drying with a hot air stream.

The corrosive solution is a 1 M hydrochloric acid solution which prepared by diluting the 37% concentrated acid with distilled water. The used concentration range of PID compound was from 10^{-6} to 10^{-3} M and its molecular structure was presented in Figure 1.

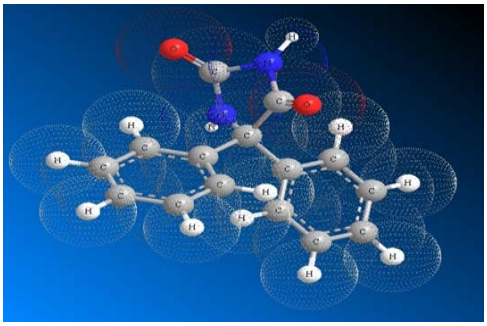

Fig. 1. Molecular structure of 5, 5-diphenylimidazolidine-2, 4-dione (PID)

2.2. The gravimetric measurement

This technique is used with a simple apparatus which is easy to implement and its principle is based on the loss of weight Δm surface samples S during the time t immersed in a corrosive solution. It consists of measuring the mass loss so as to obtain reliable and reproducible results. The mild steel substrate is subjected before each test, to a pre-treatment. The used samples are immersed vertically for 6 hours in 1 M HCl at a temperature of 298 K. The inhibition efficiency η_w was given as follows:

$$\eta_w\% = \frac{W^0_{corr} - W_{corr}}{W^0_{corr}} \times 100 \quad (1)$$

Where W^0_{corr} and W_{corr} are respectively the corrosion rates in the absence and presence of inhibitor.

2.3. Electrochemical measurements

The electrochemical measurements were carried out through the use of a Voltabab potentiostat/galvanostat PGZ 100 controlled by a computer associated with software "Voltamaster 4". For all the tests, we used a double-wall thermostated cell (Tacussel type CEC/TH) containing three electrodes: mild steel as a working electrode (1 cm^2); Platinum as an auxiliary electrode and Ag/AgCl as the reference electrode. Before each experiment, the surface of the working electrode is well treated as mentioned above. The electrode is maintained at its free corrosion potential for 30 minutes under normal aeration conditions at 298 K.

The potentiodynamic polarization curves were recorded in a potential range from – 900 mV/Ag/AgCl with a scan rate of 0.5 mV/s.

The inhibition efficiency was calculated using the following relationship:

$$\eta_{PP} = \frac{i^0_{corr} - i_{corr}}{i^0_{corr}} \times 100 \quad (2)$$

Where i_{corr}^{0} and i_{corr} are the corrosion current density values without and with inhibitor, respectively.

For the electrochemical impedance spectroscopy measurements, the frequency range is from 100 kHz to 0.1 Hz, with 10 points/decade, after 30 min of immersion using a Potentiostat/Galvanostat type PGZ 100. The ZView 2.80 software was employed to extract and to model the obtained plots. The inhibition efficiency, η_{EIS} %, was calculated according to the equation (3):

$$\eta_{EIS}(\%) = \left(\frac{R_{ct} - R_{ct}^{\circ}}{R_{ct}} \right) \times 100 \quad (3)$$

Where R_{ct}° and R_{ct} are the transfer resistance of mild steel electrode in the uninhibited and inhibited solutions, respectively.

2.4. Theoretical study

2.4.1. Calculates quantum parameters by DFT theory

The calculations of the chemical structural parameters, which are recently used in the field of corrosion, have proven their inhibition efficiency against corrosion by organic compounds [14-18]. All computations were made using the Gaussian package program. For calculations, B3LYP method, a version of the DFT methods, was employed and polarized basis sets such as 6-31G (d,p) and the Gaussian software 09W [19-21].

Geometric optimization of the PID inhibitor was also performed to determine the electron density distribution on the chemical surface of a molecule.

So, the electronegativity (χ), electron affinity values (EA) ionization potential (IE), the energy of the lowest unoccupied orbital (ELUMO), the energy of the highest occupied molecular orbital, EHOMO and gap energy (ΔEgap) of any chemical system, were interrelated as follows [22-25]:

$$\Delta E_{gap} = E_{LUMO} - E_{HOMO} \quad (4)$$

$$EI = -E_{HOMO} \quad (5)$$

$$EA = -E_{LUMO} \quad (6)$$

$$\chi = \frac{IE + EA}{2} \quad (7)$$

The overall hardness (η) and the chemical softness (σ) are given by the following relations [26]:

$$\eta = \frac{\Delta E_{gap}}{2} \tag{8}$$

$$\sigma = \frac{1}{\eta} \tag{9}$$

Therefore, the fraction of electrons transferred (ΔN) from the inhibiting molecule to the metal atom is calculated according to the following equation [27]:

$$\Delta N = \frac{\varphi - \chi_{inh}}{2\left(\eta_{Fe} + \eta_{inh}\right)} \tag{10}$$

Where ∅ and χ_{inh} represent, respectively, the working function and the absolute electronegativity of the inhibitor molecule, and η_{Fe}, η_{inh}, represent, respectively, the absolute hardness of iron and the inhibitor molecule.

So, the calculation of ΔN value is more appropriate for the use of the work function (∅). For this reason, to measure the ΔN value, χ_{Fe} is replaced by ∅. From the DFT calculations, the values obtained from ∅ are 3.91 eV, 4.82 eV and 3.88 eV for the Fe (100), (110) and (111) surfaces, respectively [28,29]. The overall hardness of Fe=0, assuming that for a metal mass I=A because they are milder than the neutral metal atoms [30].

The local responsiveness was analyzed by evaluating the Fukui indices (FI). The FI calculation is performed by the Material Studio TM software version 8 by Accelrys Inc, by using the Dmol3 module. All the calculations are performed by using the functional exchange-correlation (B3LYP) and the digital double polarization (DNP).

The condensed form of Fukui functions in a molecule with N electrons has been proposed by Yang and Mortier [31]:

$$f_k^+ = P_k(N+1) - P_k(N) \qquad \text{Nucleophilic attack} \tag{11}$$

$$f_k^- = P_k(N) - P_k(N-1) \qquad \text{Electrophilic attack} \tag{12}$$

$P_k\left(N\right)$: Electronic population of the atom k in the neutral molecule.

$P_k\left(N+1\right)$: Electronic population of the atom k in the anionic molecule.

$P_k\left(N-1\right)$: Electronic population of the atom k in the cationic molecule.

Where f_k^+ and f_k^- represent the ability of the atom k to react with a nucleophile and electrophile, respectively.

2.4.2. Monte Carlo simulation (MC)

The Monte Carlo (MC) simulations were performed so as to calculate the adsorption energy in the best adsorption configuration of an inhibitor on a clean metallic surface. In this work, the MC simulations were performed by using the Studio Material TM 8 (from Accelrys

Inc.) [32]. The Fe crystal was cleaved along the (110) plane, this is the surface the most stable, as indicated in the literature [33]. Then, the Fe (110) plane was enlarged in a super cell suitable for providing a large surface area for the inhibitor interaction. the inhibitor and Fe (110) surface was performed in a simulation box (26.89×26.89×22.13 Å) with periodic boundary conditions, after which a vacuum plate with thicknesses of 50 Å was constructed above the Fe plane (110). All simulations have been implemented with the COMPASS force field so as to optimize the structure of the system of interest [34,5].

3. RESULTS AND DISCUSSION

3.1. Weight loss measurements

The corrosion rate and inhibition efficiency values were determined at different concentrations of PID at 298K and are collated in table 1. It is clearly indicated that the corrosion rate of mild steel in the presence of PID decreases compared to uninhibited solution. As a consequence, the inhibition efficiency increases to reach a maximum value of 93.4% at 10^{-3} M. This behavior leads to blockages of existing active sites on the metal surface.

Table 1. The gravimetric results of mild steel in 1 M HCl with and without different concentrations of PID at 298 K for 6 h

Medium	**Conc. (M)**	**W_{corr} (mg cm^{-2} h^{-1})**	**η_w (%)**
Blank solution	00	1.54	_
PID	10^{-6}	0.20	86.9
	10^{-5}	0.19	87.3
	10^{-4}	0.13	91.2
	10^{-3}	0.10	93.4

3.2. Potentiodynamic polarization curves

3.2.1. Concentration effect

Figure 2 shows the potentiodynamic polarization curves of mild steel in 1 M HCl solution without and with different concentrations of PID at 298 K.

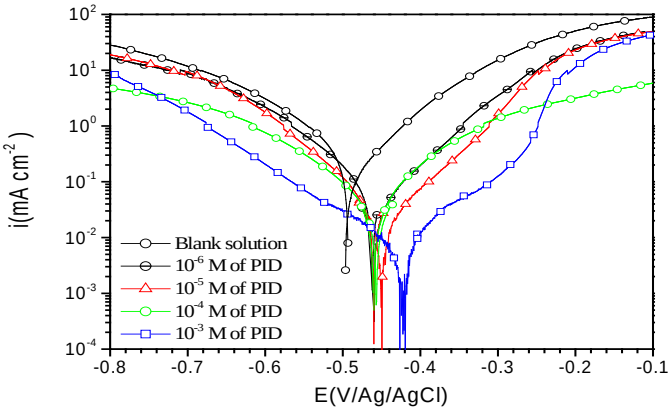

Fig. 2. Potentiodynamic polarization curves of mild steel in 1 M HCl containing different concentrations of PID at 298 K

It is noted that the cathodic and anodic polarization curves are in the Tafel lines form and the corrosion current densities decrease with inhibitor concentrations in both domains, reflecting the mixed character of the studied inhibitor. In addition, the obtained decrease is very remarkable for the optimal concentration 10^{-3} M which can be explained by the formation of a protective film. On the other hand, the formation of this film was justified by the appearance of a pseudo-plate in the anodic domain. This film was desorbed beyond the potential of E_{corr} = - 260 mV/(Ag/AgCl).

Table 2. Electrochemical polarization parameters and inhibition efficiencies of mild steel in 1 M HCl containing various concentrations of PID at 298 K

Medium	Conc. (M)	$-E_{corr}$ mV/(Ag/AgCl)	$-\beta_c$ (mV dec^{-1})	β_a (mV dec^{-1})	i_{corr} (µA cm^{-2})	η_{PP} (%)
Blank solution	00	498	92	104	983	-
PID	10^{-6}	460	90	52.1	105.18	89.4
	10^{-5}	458	82	56.5	96.33	90.2
	10^{-4}	451	68	52.8	77.65	92.1
	10^{-3}	459	62	63.8	49.15	95.0

The electrochemical parameters are regrouped in table 2. It is remarked that the addition of PID results in a decrease in the corrosion current density (i_{corr}) values. It is observed that also that the cathodic Tafel slopes (β_c) are slightly varied with PID addition indicating a simple blockage of cathodic sites with a change in the proton reduction mechanism. On the other hand, it is noted that anodic slopes are changed with the presence of PID indicating a change in the mild steel dissolution. According to the literature [36], it has been reported that

if the displacement in E_{corr} (inhibitor) is greater than 85 mV compared to E_{corr} (Blank), the inhibitor can be considered as a cathodic or anodic type; while if the displacement in E_{corr} (inhibitor) is lower than 85 mV, the inhibitor can be considered as a mixed type. In this work, the change in E_{corr} values is between 38 mV and 47 mV, so that PID compound can classify as a mixed inhibitor.

3.3. Electrochemical impedance spectroscopy

The Nyquist diagrams of mild steel in 1 M HCl solution without and with different concentrations of PID are shown in Figure 3 after 30 min of immersion at 298 K and at the open circuit potential (E_{OCP}). It is noted that the impedance spectra have a single capacitive loop indicating that the mild steel corrosion is mainly controlled by a charge transfer process [37,38]. Generally, this capacity is related to the charge transfer of the corrosion process and the behavior of the double layer. It is also observed that the loops diameter in the presence of PID increases with its concentration. In addition, remarkably, these capacitive loops are not perfect semicircles that can be attributed to the effect of the frequency dispersion. This behavior was generally related to the roughness and inhomogeneity of the metal surface [39].

The experimental impedance data are simulated an appropriate equivalent circuit shown in the Figure (4), the circuit used allows the characterization of the electrolyte resistance (R_s), the polarization resistance (R_p) and the constant phase element (CPE). The introduction of CPE in the circuit for obtaining an effective description of frequency dependence of non-ideal capacitive behavior is defined by the flowing relation (13).

$$Z_{CPE} = A^{-1}(i\omega)^{-n} \tag{13}$$

Where Q is the CPE constant in ($\Omega^{-1}s^n\ cm^{-2}$), n is the CPE exponent which can be used as a gauge of the heterogeneity or roughness of the surface (ranges from 0 to 1), $i^2=1$ is an imaginary number and w is the angular frequency (rad s^{-1}) ($\omega = 2\pi f$, where f is the frequency), the CPE is presented like an ideal double layer capacitance (C_{dl}), According to Hsu and Mansfeld [40], the values of the double layer capacitance (C_{dl}) were calculated according to following equation (14).

$$C_{dl} = \left(QR_p^{1-n}\right)^{1/n} \tag{14}$$

The derived impedance parameters are presented in Table 3.

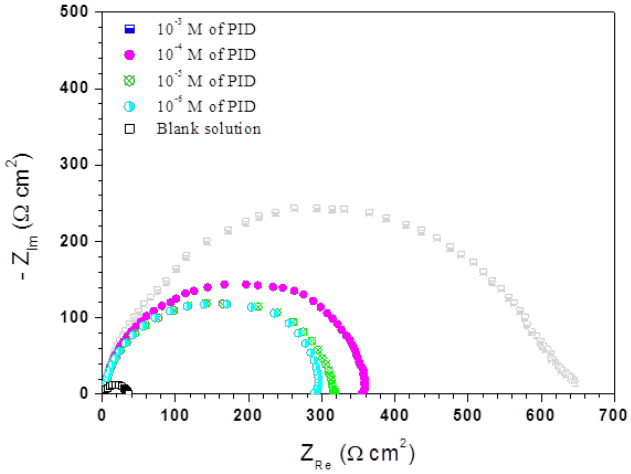

Fig. 3. Nyquist diagram of mild steel in 1 M HCl without and with different concentrations of PID at E_{OCP}

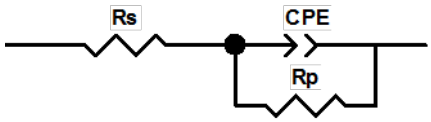

Fig. 4. Proposed equivalent electrical circuit of metal/PID/HCl

Table 3. Corrosion parameters and inhibition efficiency obtained from impedance

Medium	C (M)	R_p (Ω cm^2)	n	Q×10^{-4} ($S^n\ \Omega^{-1}$ cm^{-2})	C_{dl} (μF cm^{-2})	η_{EIS} (%)	θ
Blank solution	00	34.35	0.890	1.561	81.80	-	-
PID	10^{-6}	291.70	0.901	1.120	76.90	88.2	0.882
	10^{-5}	306.80	0.896	1.041	69.80	88.8	0.888
	10^{-4}	356.80	0.888	0.950	61.99	90.3	0.903
	10^{-3}	615.20	0.891	0.800	56.12	94.4	0.944

The data in table 3 showed that the polarization resistance R_p increases while the double layer capacitance (C_{dl}) value decreases with PID concentration. The increase in R_p was attributed to the formation of a protective film on the metallic surface and the decrease in C_{dl} can be interpreted as a decrease in the local dielectric constant and/or an increase in the thickness of the electrochemical double layer this leads to the adsorption of PID molecules on the metal surface [41]. On the other hand, the decrease in C_{d1} was consistent with the Helmholtz model given by the following equation [42]:

$$C_{dl} = \frac{\varepsilon_0 \times \varepsilon \times S}{\delta} \quad (15)$$

Where δ is the thickness of the protective layer, S is the electrode zone, ε_o is the vacuum permittivity and ε is the dielectric constant of the medium.

3.2.2. Temperature solution effect

It is known that the temperature can modify the mechanism and action mode of an inhibitor on a metallic surface. Therefore, in order to evaluate the temperature influence on inhibitor performance, the potentiodynamic polarization curves were carried out for mild steel studied in 1 M HCl without and with 10^{-3} M of PID at the temperature range from 298 K to 328 K. the obtained results are in Figure 5 and their extracted parameters are illustrated in table 4.

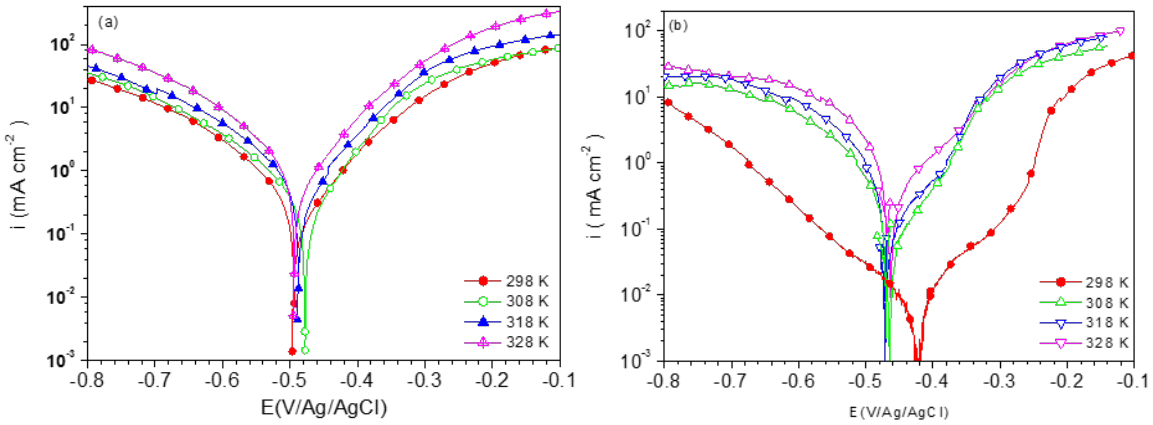

Fig. 5. Potentiodynamic polarization curves of mild steel in 1 M HCl at different temperatures (a) without and (b) with 10^{-3} M of PID

Table 4. Effect of temperature on the electrochemical parameters for mild steel in 1 M HCl without and with 10^{-3} M of PID

Medium	**T (K)**	**$-E_{corr}$ (mV/Ag/AgCl)**	**i_{corr} (µA cm^{-2})**	**η_{PP} (%)**
Blank solution	298	498	983	-
	308	491	1200	-
	318	475	1450	-
	328	465	2200	-
10^{-3} M of PID	298	459	49	95.0
	308	424	67	94.4
	318	432	243	83.2
	328	444	600	72.7

It is remarked that the current density increases with temperature in both cases which is greater in the case of the blank solution. In addition, it is noted that the corrosion potential

shifts to the cathodic direction in the case of PID while it stays constant in the case of the blank solution.

It can see from table 4 that the corrosion current density (i_{corr}) increases with increase of temperature which is greater in the case of the uninhibited solution. It is also remarked that the inhibition efficiency of PID decreases with temperature. This behavior can increase to increase the corrosion kinetics of mild steel, the PID desorption on the metal surface. In order to calculate the kinetic parameters of activation of the corrosion process of mild steel, the Arrhenius equation (16) and its alternative form (17):

$$i_{corr} = k \exp\left(-\frac{E_a}{RT}\right) \quad (16)$$

$$i_{corr} = \frac{RT}{Nh}\exp\left(\frac{\Delta S_a}{R}\right)\exp\left(-\frac{\Delta H_a}{RT}\right) \quad (17)$$

Where E_a is the apparent activation energy of corrosion, R is the perfect gas constant, k is the pre-exponential factor of Arrhenius, h is the Plank constant, T is the absolute temperature, ΔS_a is the activation entropy and ΔH_a is the activation enthalpy.

However, the apparent activation energies in the absence and presence of 10^{-3} M of PID are calculated by the plot Ln (i_{corr}) according to 1/T (Figure 6), and the obtained results are listed in table 5. As it is shown in Table 5, the increase of E_a in the presence of PID can be interpreted as a physical adsorption. Indeed, a higher energy barrier for the corrosion process in the inhibited solution is associated with adsorption to a weak chemical bond between the inhibitory molecules and the mild steel surface [43,44].

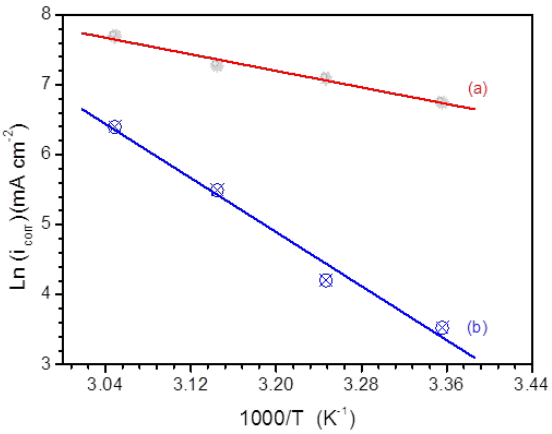

Fig. 6. Arrhenius plot of mild steel in 1 M HCl (a) the absence and (b) presence of 10^{-3} M PID at different temperatures

Szauer and Brand explained that the increase in activation energy can be attributed to an appreciable decrease in inhibitor adsorption on the metallic surface as temperature increases [45]. Figure 7 shows the variation of Ln (i_{corr}/T) according to 1000/T with a slope of (ΔH_a/R)

and an intersection of (Ln R/Nh+ΔS_a/R) from which the values of ΔH_a and ΔS_a were calculated and listed in table 5.

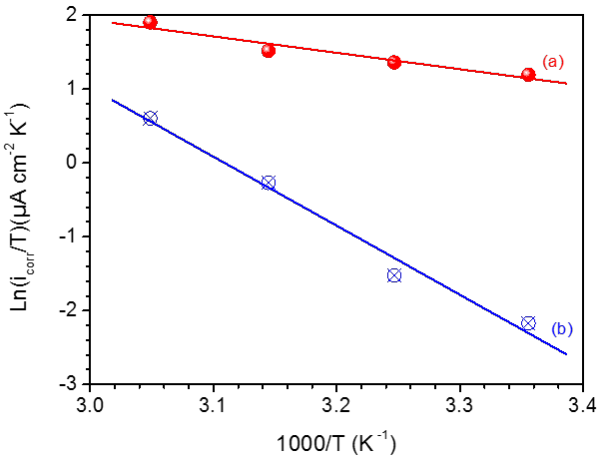

Fig. 7. Transient Arrhenius plot for mild steel in 1 M HCl in the absence and presence of 10^{-3} M PID at different temperatures

The positive values of ΔH_a in the absence and presence of PID reflect the endothermic nature of the dissolution process of mild steel. In addition, the value of ΔS_a is higher and positive for the inhibited solution than for the uninhibited solution (table 5). This has suggested that an increase in randomness occurs by passing reagents to the activated electrode/adsorbed species complex [46,47].

Table 5. Activation parameters for mild steel in 1 M HCl in the absence and presence of 10^{-3} M of PID

Medium	E_a (KJ mol^{-1})	ΔH_a (KJ mol^{-1})	ΔS_a (J mol^{-1} K^{-1})
Blank solution	21.05	18.45	-126.08
10^{-3} M of PID	80.27	77.68	43.98

3.3.2. The adsorption isotherm

The adsorption of the inhibitor molecules on the metal/solution interface is a substitution process, which can allow us to give a view of the adsorption mechanism of the investigated inhibitor on the metallic surface [48,49]. Several adsorption isotherms were evaluated and the Langmuir adsorption isotherm remains the best description of the studied inhibitor adsorption behavior. The surface coverage values, θ (θ=(η_{EIS} /%)/100), for different concentrations of PID were used to explain the best adsorption isotherm. This can be expressed by the following equation (18) [50]:

$$\frac{C_{\text{inh}}}{\theta} = \frac{1}{K_{\text{ads}}} + C_{\text{inh}} \quad (18)$$

Where C_{inh} is the inhibitor concentration and K_{ads} is the adsorption constant.

It is found that the ratio of the variation of C_{inh}/θ according to C_{inh} gives a straight line with a slope close to unity. This indicates that the adsorption of PID inhibitor on the mild steel surface obeys the Langmuir adsorption isotherm.

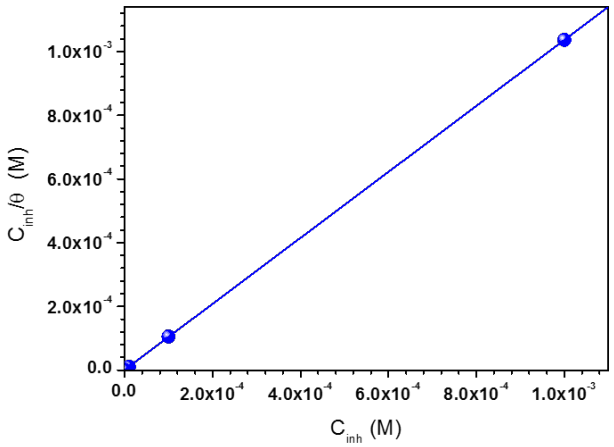

Fig. 8. Langmuir inhibitor adsorption on the mild steel surface 1 M HCl at 298 K

The free adsorption enthalpy change ΔG°_{ads} was calculated by using the following expression [51]:

$$\Delta G^{\circ}_{ads} = -RTLn\left(55.5K_{\text{ads}}\right) \quad (19)$$

Where R is the gas constant, 55.5 is the solution water concentration and T is the absolute temperature. It is found that the value of ΔG°_{ads} equal to -45.32 kJ mol^{-1}.

Generally, if the values of are close to or greater than -20 kJ/mol, they are related to electrostatic interactions, for the values of which are close to -40 kJ/mol or inferiors imply the formation of the bonds of the chemical nature between the molecules of the inhibitor and the metal surface. For the values of lie -20 kJ/mol and -40 kJ/mol both phenomena applying at the same time [41,42]. The large value of ΔG°_{ads} and its negative sign is usually characteristic of strong interaction and a highly efficient adsorption. The high value of shows that in the presence of 1 M HCl chemisorption of PID may occur. The possible mechanisms for chemisorption can be attributed to the donation of π-electron in the aromatic rings, the presence of two oxygen and two nitrogen atoms in inhibitor molecule as reactive centers is an electrostatic adsorption of the protonated inhibitor in acidic solution to adsorb on the metal surface [52,53].

3.4. Theoretical study

3.4.1. Density Functional Theory (DFT)

3.4.1.1 Calculation of the main structural parameters of PID compound

In order to correlate the obtained experimental results with the electronic properties of PID compound, a theoretical study was carried out at the B3LYP/6 -31G (d, p) level using Gaussian 09 software. The quantum theoretical calculation makes it possible to identify the different quantum structural parameters. It is known that the HOMO energy is often associated with the ability of the molecule to transfer its electrons to suitable vacant orbitals. Thus, the high E_{HOMO} values of the inhibitor indicate its tendency to donate electrons to an acceptor with an empty molecular orbital; consequently; facilitates its adsorption. On the other hand, the energy of LUMO informs on the acceptor character of electrons of the molecule. Decreasing the E_{LUMO} value is an indicator of the molecule's ability to accept electrons [54,55].

The optimized structure of the tested molecule with the electronic densities HOMO and LUMO were represented in Figure 9.

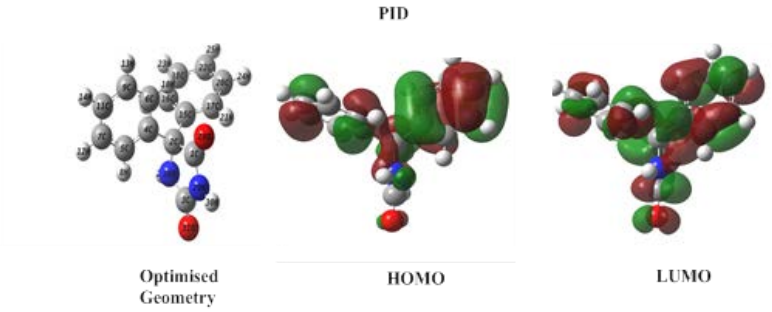

Fig. 9. Optimized molecular structure of PID with HOMO and LUMO electronic densities

Table 6. Calculated quantum parameters of PID molecules

E_{LUMO} (eV)	E_{HOMO} (eV)	ΔE_{gap} (eV)	η (eV)	σ (e V^{-1})	IE (eV)	χ (eV)	EA (eV)	ΔE_b (eV)	ΔN_{110}	TE (eV)
-0.707	-6.674	5.967	2.983	0.335	6.674	3.372	0.707	-0.745	0.242	-22825.47

It is observed that the HOMO and LUMO density distribution is located over the entire studied inhibitor surface. This result indicates that PID has sites available for nucleophilic and electrophilic attack. The main quantum parameters are collected in table 6.

It can be shown from table 6 that the tested inhibitor has a high energy HOMO (- 6.674 eV) and low energy LUMO (-0.707 eV), as well as a low energy gap ΔE_{gap} (5.967 eV) which reinforces its inhibitory action on the metal surface. So, the electrons transferred number (ΔN_{110}) from PID molecules to mild steel surface was in the order of 0.242. According to the Lukovits study [56], if the value of $\Delta N<3.6$, the inhibitory performance is good. In our case, ΔN_{110} is lower than the limit value set by Lukovits indicating that the PID is a good inhibitor for mild steel in 1 M HCl. It is also found that the PID has negative feedback energy ΔE_b=-0.745 eV which can be indicated that this compound can accept electrons from the mild steel surface.

3.4.2. Determination of Active PID inhibitor Sites

3.4.2.1. Mulliken charge method and electronic total density of PID compound

In order to determine the active sites of the PID molecules, the Mulliken charges and the total electron density were evaluated. Atoms with negative charges are those with high electron density. These atoms (sites) therefore behave like nucleophilic centers when they interact with the metal surface. Figure 10 shows the Mulliken charges distribution of atoms and total density mapped to the molecular structure. It can be seen that the oxygen, nitrogen and certain carbon atoms have high charge densities. These atoms are the active centers that have the greatest ability to bind to the metal surface [57].

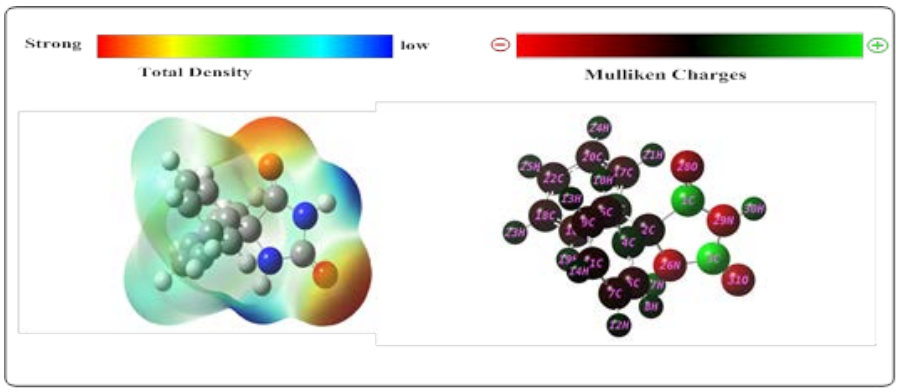

Fig. 10. Distribution of total mapped electron density and Mulliken charges of PID compound.

Table 7. Mulliken charge distribution of PID inhibitor

Atoms	**1 C**	**2 C**	**3 C**	**4 C**	**5 C**	**6 C**	**7 C**	**9 C**	**11 C**	**15 C**
Mulliken charges	0.620	-0.047	0.746	0.110	-0.118	-0.089	-0.089	-0.096	-0.079	0.136
Atoms	**16 C**	**17 C**	**18 C**	**20 C**	**22 C**	**26 N**	**28 O**	**29 N**	**31 O**	

Mulliken charges	-0.120	-0.116	-0.090	-0.094	-0.078	-0.556	-0.485	-0.574	-0.496

On the other hand, some carbon atoms carry positive charges which can have a low density and these sites can attack by nucleophilic groups. Therefore the PID can accept and give electrons through these active centers. The distribution of Mulliken charges is summarized in table 7.

3.4.2.2. The local reactivity of the studied PID (Fukui indices)

Generally, the local reactivity is analyzed by using Fukui's condensed function. The latter allowed us to determine the atoms which are responsible for an electrophilic or nucleophilic attack [58, 59]. Fukui indices calculated for the PID inhibitor are shown in table 8.

Table 8. Fukui indices calculated for the PID compound using the function GGA/BOP with the low DNP (3.5)

Atoms	**C1**	**C2**	**C3**	**C4**	**C5**	**C6**	**C7**	**C9**	**C11**	
f_k^+	0.128	0.128	0.038	0.007	0.005	0.018	0.016	0.008	0.039	
f_k^-	0.011	-0.004	0.015	0.028	0.027	0.023	0.028	0.016	0.052	
Atoms	**C15**	**C16**	**C17**	**C18**	**C20**	**C22**	**N26**	**O28**	**N29**	**O31**
f_k^+	0.002	0.012	-0.003	0.011	0.020	0.017	0.016	0.127	0.017	0.096
f_k^-	-0.001	0.010	-0.000	0.010	0.025	0.025	0.007	0.100	0.018	0.073

It is shown from table 8 that the compound PID has the highest values which are located on the atoms C1, C2, O28, and O31. These sites can be accepted electrons from the mild steel surface. So, the atoms C11, O28, and O31 are capable of giving electrons.

3.4.3. The impact of protonation on the main structural parameters of the studied neutral molecule

The organic molecules have several active centers available for protonation acidic medium. So, the PID compound is very likely to be protonated at several sites, such as N26, O28, N29, and O31. Among these sites, atom O31 is the most favorable center for protonation. This choice was based on two considerations: firstly, this site has a considerable negative Mulliken charge; secondly, this atom has a high total density.

The representation of the distribution of the electron density HOMO and the total density charge mapped of protonated and unprotonated PID compound are shown in Figure 11. From this Figure, it is clear that the low total electron density which is represented by a blue color is the positive region and was distributed over all the surface of the protonated molecule.

These observations indicate that the protonated PID(H^+) molecule exhibits more reactive characters with mild steel surface in acid medium.

However, the distribution of HOMO electron density of neutral and protonated PID(H^+) compound is also shown in Figure 11. It is noted that the HOMO density is a little less with a comparison to neutral form. Thus, after protonation of PID, the total density mapped appeared on its surface when the backsides were empty in neutral form. This result indicates that the protonated form might become very reactive

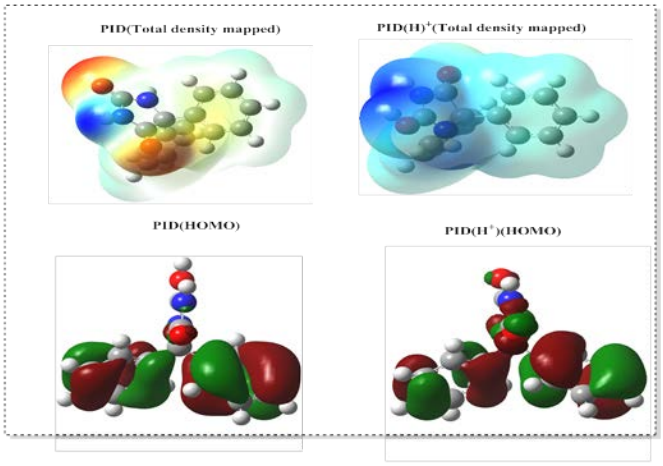

Fig. 11. Distribution of total mapped and HOMO density of protonated and unprotonated PID

Table 9 represents the principal quantum parameters values of the protonated and unprotonated of PID.

Table 9. Principal quantum parameters values of protonated and unprotonated PID

Inhibitors	**E_{LUMO} (eV)**	**E_{HOMO} (eV)**	**ΔEgap (eV)**	**ΔN_{110} (eV)**
PID	-0.707	- 6.674	5.967	0.242
PID (H^+)	- 4.489	- 9.830	5.341	- 2.340

It is shown from table 9 that the E_{HOMO} value of protonated PID shifts to more negative values compared to for the neutral form of PID. This result indicated that the electron donor capacity of PID decreases after protonation [60,61]. Moreover, this phenomenon is supported by the electrons transferred number (ΔN_{110}) between the inhibitor molecules and mild steel surface. In addition, it is observed that all the calculated ΔN_{110} values for surface Fe (1 1 0) are negative. This means that donating electrons from inhibitors to the metal surface is no longer possible [62].

Therefore, the protonation of PID compound indicated that this compound has vacant orbital's available to accept electrons. This result confirms the method used by Fukui indices and Mulliken's charge of atoms.

3.4.4. The Monte Carlo simulation study

In order to study the interactions between an organic molecule and a metal surface, Monte Carlo simulation (MC) was used. This method is a modern way to consider the most stable configuration of adsorption [63,64].

The lateral and upper views of the best low-energy, more stable adsorption configuration of PID compound on the Fe (110) surface by using MC simulations are shown in Figure 12. It is noted that the PID adsorbs parallel at iron surface.

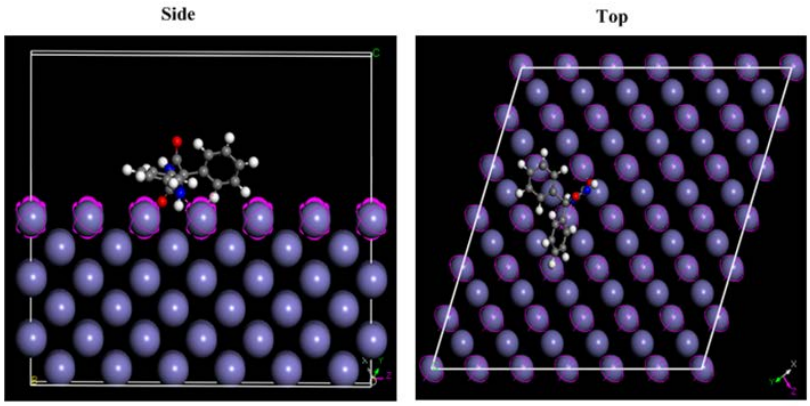

Fig. 12. Top and side views of the most stable adsorption configurations of PID at the iron surface

The different descriptors and outputs calculated from MC simulation for PID are summarized in table 10. It can be concluded that the adsorption energy (E_{ads}) is negative and strong which indicates that the adsorption of PID on the iron surface is well noticed [65-68]. It is found that there is a good agreement between the quantum chemical parameters and the MC outputs.

Table 10. Outputs and descriptors calculated from Monte Carlo simulations of the best stable adsorption configuration of PID on Fe (110) surface (all in kcal mol^{-1})

Structures	Total energy (E_T)	Adsorption energy (E_{ad})	Rigid adsorption energy (E_{ra})	Deformation energy (E_{def})	PID: dE_{ad}/dN_i
Fe (1 1 0) (2) – 1	-115.149	-59.559	-48.679	-10.8790	-59.559
Fe (1 1 0) (2) – 2	-114.441	-58.850	-49.142	-9.708	-58.850
Fe (1 1 0) (2) – 3	-113.007	-57.417	-47.557	-9.859	-57.417
Fe (1 1 0) (2) – 4	-112.178	-56.587	-46.208	-10.378	-56.587
Fe (1 1 0) (2) – 5	-111.679	-56.088	-45.805	-10.283	-56.088
Fe (1 1 0) (2) – 6	-111.293	-55.702	-44.607	-11.094	-55.702
Fe (1 1 0) (2) – 7	-111.066	-55.475	-44.291	-11.184	-55.475
Fe (1 1 0) (2) – 8	-110.850	-55.260	-44.083	-11.176	-55.260
Fe (1 1 0) (2) – 9	-110.214	-54.623	-43.270	-11.352	-54.623
Fe(1 1 0) (2) – 10	-110.006	-54.415	-43.505	-10.910	-54.415

The adsorption density of inhibitor molecules (PID) on a metallic surface is given in Figure 13. It is shown that PID is likely to adsorb on the iron surface (110) to form stable organic adsorption layers, and can be seen as a barrier to protect metal surface from corrosion.

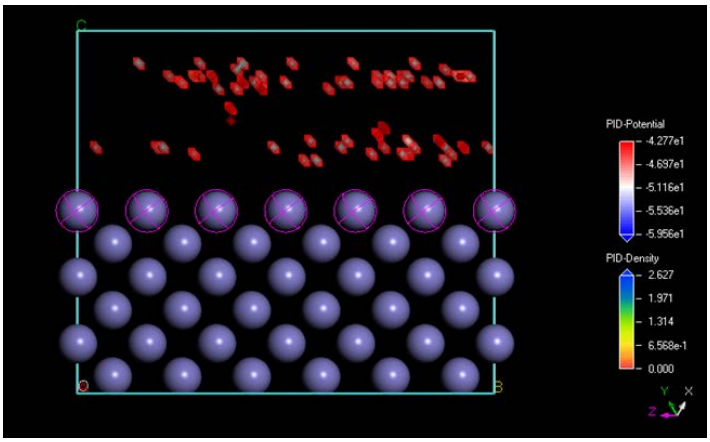

Fig. 13. Adsorption density field for Fe (110)/PID interface obtained through the Monte Carlo simulation

3.5. Inhibition mechanism of PID

In acidic solutions, the organic molecules inhibit mild steel corrosion phenomenon by adsorption on metal/electrolyte interface. In this sense, it has chosen to propose a simple acceptable inhibition mechanism based on both experimental and theoretical results.

In hydrochloric acid, the PID compound can exist in the protonated form in equilibrium with its corresponding molecular form:

$$PID + HCl \leftrightarrow PIDH^{+} + Cl^{-}$$

So, the electrostatic interactions are the first step in the adsorption of the test compound. Indeed, cationic adsorption of $PIDH^{+}$ will be favored by the concentration of Cl^{-} anions on the metal surface [69]. Therefore, the chemical adsorption is done by donor interactions between the free electron pairs of heteroatoms (N, O) and the unoccupied orbital of the iron atoms. Finally, the bonds of the retrodonation occur by electron transfer from the orbit of iron to the vacant π* orbital (anti-binding) of PID molecule [70,71].

According to this study, the mode of adsorption of PID inhibitor on the mild steel surface can be described by the diagram presented in Figure 14.

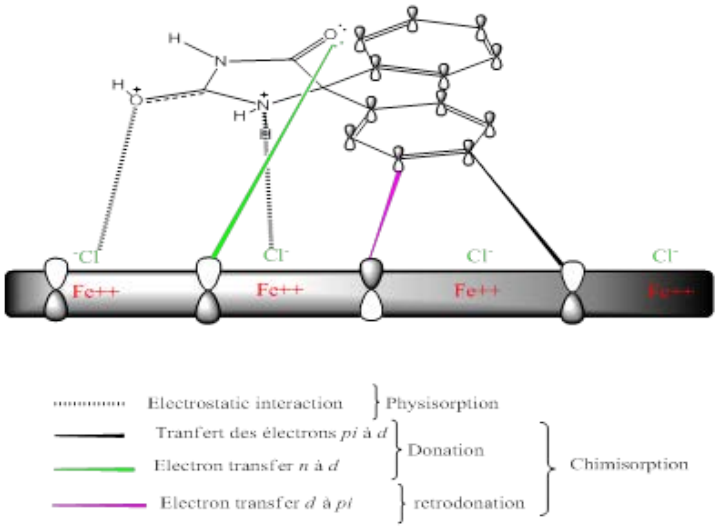

Fig. 13. Adsorption scheme of PID inhibitor on mild steel in 1 M HCl medium

4. CONCLUSION

The inhibition of mild steel corrosion was achieved by PID compound in 1 M HCl medium using various experimental and theoretical techniques. The results obtained show that the PID inhibitor is a good inhibitor for mild steel in acidic medium and it is considered a mixed type inhibitor. The impedance spectroscopy was composed by one capacitive loop which is controlled by the charge transfer process. The increase in temperature leads a

decrease in the inhibition efficiency of the studied compound. In addition, the adsorption of PID molecules on the mild steel surface in HCl solution was performed according to the Langmuir isotherm. On the other hand, the calculations of quantum parameters for PID are well correlated with the inhibition efficiency of the experimental study. The adsorption of PID on the metallic surface of the low energy iron was performed in a parallel manner and according to the Monte Carlo simulation. This result indicates that this inhibitor is well adsorbed on the mild steel surface. Finally, the experimental and theoretical results are in good agreement taking into consideration both the Fukui indices and the molecular charges by Mullikin**.**

REFERENCES

[1] M. A. Quraishi, and R. Sardar, Corrosion 58 (2010) 748.
[2] S. A. Abd El-Maksoud, and A. S. Fouda, Mater. Chem. Phys. 93 (2005) 84.
[3] M. A. Migahed, and I. F. Nassar, Electrochim. Acta 53 (2008) 2877.
[4] V. S. Sastri, and J. R. Perumareddi, Corros. Sci. 53 (1997) 617.
[5] I. Ahamad, R. Prasad, and M. A. Quraishi, Corros. Sci. 52 (2010) 3033.
[6] M. Masoud, M. Awad, M. Shaker, and M. El-Tahawy, Corros. Sci. 52 (2010) 2387.
[7] M. Belayachi, H. Serrar, H. Zarrok, A. El Assyry, A. Zarrouk, H. Oudda, S. Boukhris, B. Hammouti, E. E. Ebenso, and A. Geunbour, Int. J. Electrochem. Sci. 10 (2015) 3010.
[8] R. Hasanov, S. Bilge, and S. Bilgic, Corros. Sci. 52 (2010) 984.
[9] N. Eddy, Mol. Simulat.36 (2010) 354.
[10] H. Wang, X. Wang, and H. Wang, J. Mol. Model. 13 (2007) 147.
[11] Y. El Ouadi, F. Abrigach, A. Bouyanzer, R. Touzani, O. Riant, B. El Mahi, A. El Assyry, S. Radi, A. Zarrouk, and B. Hammouti, Der Pharm. Chem. 7(8) (2015) 265.
[12] S. Umoren, and U. Ekanem, Chem. Eng. Comm. 197 (2010) 1339.
[13] Y. Elaoufir, H. Bourazmi, H. Serrar, H. Zarrok, A. Zarrouk, B. Hammouti, A. Guenbour, S. Boukhriss, and H. Oudda, Der Pharm. Lett. 6 (2014) 526.
[14] M. Quraishi, R. Sardar, Mater. Chem. Phys. 78 (2003) 425.
[15] A. Stoyanova, G. Petkova, and S. Peyerimhoff, Chem. Phys. 279 (2002) 1.
[16] N. Obi-Egbedi, K. Essien, I. Obot, and E. Ebenso, Int. J. Electrochem. Sci. 6 (2011) 913.
[17] M. Ozcan, I. Dehri, and M. Erbil, Appl. Surf. Sci. 236 (2004) 155.
[18] M. Amin, M. Ahmed, H. Arida, F. Kandemirli, M. Saracoglu, T. Arslan, and M. Basaran, Corros. Sci. 53 (2011) 1895.
[19] Gaussian 03, Revision B.03, M. J. Frisch, G.W. Trucks, H. B. Schlegel, G. E. Scuseria, M. A. Robb, J. R. Cheeseman, J. A. Montgomery, Jr., T. Vreven, K. N. Kudin, J. C.

Burant, J. M. Millam, S. S. Iyengar, J. Tomasi, V. Barone, B. Mennucci, M. Cossi, G. Scalmani, N. Rega, G. A. Petersson, H. Nakatsuji, M. Hada,M. Ehara, K. Toyota, R. Fukuda, J. Hasegawa, M. Ishida, T. Nakajima, Y. Honda, O. Kitao, H. Nakai, M. Klene, X. Li, J.E. Knox, H. P. Hratchian, J. B. Cross, C. Adamo, J. Jaramillo, R. Gomperts, R. E. Stratmann, O. Yazyev, A. J. Austin, R. Cammi, C. Pomelli, J. W. Ochterski, P. Y. Ayala, K. Morokuma, G. A. Voth, P. Salvador, J. J. Dannenberg, V. G. Zakrzewski, S. Dapprich, A. D. Daniels, M. C. Strain, O. Farkas, D. K. Malick, A. D. Rabuck, K. Raghavachari, J.B. Foresman, J. V. Ortiz, Q. Cui, A. G. Baboul, S. Clifford, J. Cioslowski, B. B. Stefanov, G. Liu, A. Liashenko, P. Piskorz, I. Komaromi, R.L. Martin, D. J. Fox, T. Keith, M. A. Al-Laham, C. Y. Peng, A. Nanayakkara, M. Challacombe, P. M. W. Gill, B. Johnson, W. Chen, M. W. Wong, C. Gonzalez, J. A. Pople, Gaussian, Inc., Pittsburgh PA. (2003).

[20] G. A. Petersson, A. Bennett, T. G. Tensfeldt, M. A. Al-Laham, W. A. Shirley, and J. Mantzaris, J. Chem. Phys. 89 (1988) 2193.

[21] L. M. Vracar, and D. M. Drazic, Corros. Sci. 44 (2002) 1669.

[22] K. R. Ansari, and M. A. Quraishi, J. aiwan, Inst. Chem. Eng. 54 (2015) 145.

[23] F. Neese, An Ab initio, DFT and Semiempirical SCF-MO Package, Version 2.9; Max Planck Institute for Bioinorganic Chemistry, Mulheim an der Ruhr, Germany, Jan (2012).

[24] D. A. Becke, J. Chem. Phys. 84 (1986) 4524.

[25] C. Lee, W. Yang, and G. R. Parr, Phys. Rev. B 37 (1988) 785.

[26] S. K. Saha, A. Hens, A. RoyChowdhury, A. K. Lohar, N. C. Murmu, and P. Banerjee, Can. Chem. Trans. 2 (2014) 489.

[27] S. K. Saha, P. Ghosh, A. Hens, N. C. Murmu, and P. Banerje, Physica E 66 (2015) 332.

[28] S. Martinez, Mater. Chem. Phys. 77 (2003) 97.

[29] Z. Cao, Y. Tang, H. Cang, J. Xu, G. Lu, and W. Jing, Corros. Sci. 83 (2014) 292.

[30] A. Kokalj, Chem. Phys. 393 (2012) 1.

[31] W. Yang, and W. J. Mortier, J. Am. Chem. Soc. 108 (1986) 5708.

[32] Materials Studio., Revision 6.0. Accelrys Inc., San Diego, USA (2013).

[33] C. Verma, E. E. Ebenso, I. Bahadur, I. B. Obot, and A. M. Quraishi, J. Mol. Liq. 212(2015) 209.

[34] Y. A. Musa, T. R. Jalgham, and B. A. Mohamad, Corros. Sci. 56 (2012) 176.

[35] S. Kaya, B. Tüzün, C. Kaya, and B. I. Obot, J. Taiwan Inst. Chem. Eng. 58 (2016) 528.

[36] M. El Faydy, M. Galai, A. El Assyry, A. Tazouti, R. Touir, B. Lakhrissi, M. Ebn Touhami, and A. Zarrouk, J. Mol. Liq. 219 (2016) 396.

[37] D.B. Hmamou, R. Salghi, A. Zarrouk, H. Zarrok, R. Touzani, B. Hammouti, and A. El Assyry, J. Environ. Chem. Eng. 3 (2015) 2031.

[38] H. Zarrok, A. Zarrouk, R. Salghi, M. Ebn Touhami, H. Oudda, B. Hammouti, R. Touir, F. Bentiss, and S. S. Al-Deyab, Int. J. Electrochem. Sci. 8 (2013) 6014.
[39] M. Lebrini, M. Lagrenee, H. Vezin, M. Traisnal, and F. Bentiss, Corros. Sci. 49 (2009) 2254.
[40] C. H. Hsu, and F. Mansfeld, Corrosion 57 (2001) 747.
[41] J. Fu, S. Li, Y. Wang, L. Cao, and L. Lu, J. Mater. Sci. 45 (2010) 6255.
[42] K. F. Khaled, and M. M. Al-Qahtani, Mater. Chem. Phys. 113 (2009)150.
[43] A. Popova, E. Sokolova, S. Raicheva, and M. Christov, Corros. Sci. 45 (2003) 33.
[44] X. Li, and G. Mu, Appl. Surf. Sci. 252 (2005) 1254.
[45] T. Szauer, and A. Brandt, Electrochim. Acta 26 (1981) 1219.
[46] A. Zarrouk, B. Hammouti, A. Dafali, and F. Bentiss, Ind. Eng. Chem. Res. 52 (2013) 2560.
[47] B. Ateya, B. E. El-Anadouli, and F. M. El-Nizamy, Corros. Sci. 24 (1984) 509.
[48] G. Moretti, F. Guidi, and F. Fabris, Corros. Sci. 76 (2013) 206.
[49] S. Kharchouf, L. Majidi, M. Bouklah, B. Hammouti, A. Bouyanzer, and A. Aouniti, Arab. J. Chem. 7 (2014) 680.
[50] R. Solmaz, Corros. Sci. 81 (2014) 75.
[51] N. A. Negm, Y.M. Elkholy, M. K. Zahran, and S. M. Tawfik, Corros. Sci. 52 (2010) 3523.
[52] H. Tayebi,H. Bourazmi, B. Himmi, A. El Assyry, Y. Ramli, A. Zarrouk, A. Geunbour, B. Hammouti, Der Pharm. Chem. 6(5) (2014) 220.
[53] H. Tayebi, H. Bourazmi, B. Himmi, A. El Assyry, Y. Ramli, A. Zarrouk, A. Geunbour, B. Hammouti, and E. E. Ebenso, Der Pharm. Lett. 6 (2014) 20.
[54] D. Ben Hmamou, M. R. Aouad, R. Salghi, A. Zarrouk, M. Assouag, O. Benali, M. Messali, H. Zarrok, and B. Hammouti, J. Chem. Pharm. Res. 4 (2012) 3498.
[55] D. Wang, D. Yang, D. Zhang, K. Li, L. Gao, and T. Lin, Appl. Surf. Sci. 357 (2015) 2176.
[56] I. Lukovits, E. Kálmán, and F. Zucchi, Corros. Sci. 57 (2001) 3.
[57] A. Y. Musa, A. H. Kadhum, A. B. Mohamad, A. B. Rahoma, and H. Mesmari, J. Mol. Struct. 969 (2010) 233.
[58] S. K. Saha, M. Murmu, and P. Banerjee, J. Mol. Liq. (2016).
[59] N. O. Eddy, H. Momoh-Yahaya, and E. E. Oguzie, J. Adv. Res. 6 (2015) 203.
[60] N. A. Wazzan, I. B. Obot, and S. Kaya, J. Mol. Liq. 221 (2016) 579.
[61] S. K. Saha, M. Murmu, and P. Banerjee, J. Mol. Liq. 224 (2016) 899.
[62] S. K. Saha, A. Dutta, P. Ghosh, D. Sukul, and P. Banerjee, Phys. Chem. Chem. Phys. 18 (2016) 17898.
[63] I. B. Obot, N. O. Obi-Egbedi, E. E. Ebenso, A. S. Afolabi, and E. E. Oguzie, Res. Chem. Intermed. 39 (2013) 1927.

[64] L. Feng, H. Yang, and F. Wang, Electrochim. Acta 58 (2011) 427.
[65] I. B. Obot, S. A. Umoren, Z. M. Gasem, R. Suleiman, and B. El Ali, J. Ind. Eng. Chem. 21 (2015)1328.
[66] J. Tan, L. Guo, T. Lv, and S. Zhang, Int. J. Electrochem. Sci. 10 (2015) 823.
[67] L. Guo, S. Zhu, S. Zhang, Q. He, and W. Li, Corros. Sci. 87 (2014) 366.
[68] A. M. Kumar, R. S. Babu, I. B. Obot, and M. G. Zuhair, RSC Adv. 5 (2015) 19264.
[69] M. Lagrenee, B. Mernari, M. Bouanis, M. Traisnel, and F. Bentiss, Corros. Sci. 44 (2002) 573.
[70] R. Solmaz, G. Kardaş, B. Yazıcı, and M. Erbil, Colloids Surf. Physicochem. Eng. Asp. 312 (2008) 7.
[71] A. Dandia, S. Gupta, P. Singh, and M. Quraishi, ACS Sustain. Chem. Eng. 1 (2013) 1303.